A scintillation proximity assay for histone demethylases.

Wenyu Yu[1], Mohammad S. Eram[1], Taraneh Hajian[1], Aleksandra Szykowska[3], Nicola Burgess-Brown[3], Masoud Vedadi[1,2] and Peter J. Brown[1*]

[1]Structural Genomics Consortium, University of Toronto, 101 College Street, Toronto, ON M5G 1L7, Canada
[2]Department of Pharmacology and Toxicology, University of Toronto, 1 King's College Circle, Toronto, Ontario, M5S 1A8, Canada.
[3]Structural Genomics Consortium, University of Oxford, Oxford OX3 7DQ, United Kingdom.

Short Title: **SPA for histone demethylases**

*Corresponding Author. Phone: +1 416 978 7408; Fax: +1 416 946 0588
Email: peterj.brown@utoronto.ca

Subject category: Enzymatic Assays and Analyses

ABSTRACT

Covalent modifications, such as methylation and demethylation of lysine residues in histones, play important roles in chromatin dynamics and the regulation of gene expression. The lysine demethylases (KDMs) catalyze the demethylation of lysine residues on histone tails and are associated with diverse human diseases, including cancer, and are therefore proposed as targets for the therapeutic modulation of gene transcription. High-throughput assays have been developed to find inhibitors of KDMs, most of which are fluorescence-based assays. Here we report the development of a coupled scintillation proximity assay (SPA) for 3 KDMs: KDM1A (LSD1), KDM3A (JMJD1A) and KDM4A (JMJD2A). In this assay methylated peptides are first demethylated by a KDM, and a protein methyltransferase (PMT) is added to methylate the resulting peptide with tritiated SAM. The enzyme activities were optimized and kinetic parameters were determined. These robust coupled assays are suitable for screening KDMs in 384-well format (Z'-Factors of 0.70-0.80) facilitating discovery of inhibitors in the quest for cancer therapeutics.

Keywords

Lysine demethylases (KDMs)

Protein methyltransferases (PMTs)

KDM1A (LSD1)

KDM3A (JMJD1A)

KDM4A (JMJD2A)

Scintillation proximity assay (SPA)

Covalent histone modifications, including acetylation, methylation, phosphorylation, ubiquitinylation and sumoylation, play an important role in regulating chromatin dynamics and function [1]. Lysine residues in histones are methylated and demethylated by sequence-specific methyltransferases and demethylases which are important processes in the control of chromatin structure and transcriptional activity. There are at least 60 protein methyltransferases (PMTs) encoded in the human genome, including 51 lysine methyltransferases (PKMTs) and 9 protein arginine methyltransferases (PRMTs)[1]. Methyltransferases recognize specific protein sequences and mono-, di-, or trimethylate specific lysines or mono- or dimethylate arginine residues. Examples include EHMT2 that specifically mono- and dimethylates Lys-9 of histone H3 (H3K9) in euchromatin [2], and KMT3A specifically mono-, di-, and trimethylates Lys-36 of histone H3 (H3K36) [3].

In contrast, the lysine demethylases (KDMs) “erase” the methyl marks. There are two main classes of histone demethylases which are defined by their mechanisms: flavin adenine dinucleotide (FAD)-dependent demethylases (eg; KDM1A, KDM1B), and 2-oxoglutarate (2-OG)-dependent demethylases (eg; KDM3A and KDM4A) [4]. KDM1A, also referred to as LSD1, specifically demethylates mono- or dimethylated H3K4 and H3K9 *via* a redox process [5]. Recent evidence shows that KDM1A plays an important role in a variety of biological processes, including cell proliferation [6], adipogenesis [7], chromosome segregation and embryonic development [8, 9]. Furthermore, KDM1A can also promote tumor development by inhibiting the tumor suppressor activity of p53 [10, 11] and KDM1A inhibitors have shown anticancer effects in cells [12, 13], supporting their potential as cancer drugs [14, 15].

Another class of histone demethylases is the Jumonji domain containing histone demethylases (JKDMs). These JKDMs are Fe^{2+} and 2-oxoglutarate (2-OG)-dependent oxygenases. Members of this class constitute the largest family of lysine demethylases. In contrast to KDM1A, which is only able to demethylate mono- and dimethylated lysine residues, JKDMs are able to demethylate mono-, di- and trimethylated lysines. Although these KDMs have highly conserved methylated lysine binding pockets and act *via* a similar catalytic mechanism, they show differences in both degree and sequence specificity in their demethylation reactions [16]. For instance, the KDM4 subfamily (KDM4A, KDM4B, KDM4C, and KDM4D) act on di- and trimethylated H3K9, H3K36, H1K26, while the KDM2 subfamily (KDM2A and KDM2B) only acts on mono- and dimethylated H3K36 [17]. This subfamily is linked to a variety of cancers [4], and a small molecule JKDM modulator has been shown to selectively inhibit cancer growth [18].

Because of the potential pharmaceutical significance of KDM inhibitors, high-throughput assays have been developed to find small molecule modulators of KDM activity and several commercial assay kits are available [19-22]. Most of these assays and kits use a fluorescence-based format and require no wash or liquid transfer steps, and the homogeneous “mix-and-measure” nature makes these assays simple and robust with relatively low cost. However, these assays usually tend to generate a high number of false positives because of fluorescence interference from labeled substrates, colored and fluorescent compounds, and fluorescent tracers [23-25]. High-throughput mass spectrometry has been used to overcome these shortcomings [26], and is widely used as a confirmatory assay for KDMs [20], however, this technique has inherent throughput

limitations. The ability of LC/MS to separate substrates containing different methylation states is another important consideration and is vital when screening involves the detection of multiple chemical entities [27].

The scintillation proximity assay (SPA) is a homogeneous, versatile assay technology for the rapid and sensitive analysis of a wide range of biological processes. The assay gives fewer false positives, is widely recognized as the "gold standard" for radiometric high-throughput screening [28, 29], and has been used for histone methyltransferases (HMTs) [30-32]. Here we report the development of coupled SPA methods for 3 KDMs. In this assay, biotin-labeled methylated peptides are demethylated by a KDM, and subsequently a protein methyltransferase is added to methylate the peptide product with ^{3}H-SAM after KDMs are quenched by heat shock. We also characterized the kinetic parameters and highlight the broader utility of this approach as a generic assay for all KDMs.

Materials and methods

Iron (II) sulfate (Cat#: F7002), 2-OG (Cat#: K1875), ascorbic acid (Cat#: A5960) and S-(5'-Adenosyl)-L-methionine (referred to as "cold SAM"; Cat#: 2408) were purchased from Sigma-Aldrich. Tritiated SAM ("hot SAM"; Cat #: NET155V250UC) and 384-well FlashPlate coated with Streptavidin (Cat#: SMP410A001PK) were from PerkinElmer. KDM1A (Cat #:50097; purity: ~ 80%) was from BPS bioscience. Biotin-labeled H3K4me1(1-21) (sequence: ARTK(me)QTARKSTGGKAPRKQLA-GGK-Biotin), H3K9me2(1-21) (sequence: ARTKQTARK(me2)STGGKAPRKQLA-GGK-Biotin),

H3K9me3(1-21) (sequence: ARTKQTARK(me3)STGGKAPRKQLA-GGK-Biotin) were from AnaSpec. Inhibitors RN-1 and IOX1 were obtained from Sigma-Aldrich.

Protein expression and purification

DNA fragments encoding human EHMT2 residues 913-1193, and KMT1B residues 52-350 were amplified by PCR and sub-cloned into the SGC in-house pET28a-LIC vector. For KMT7, a DNA fragment encoding residues 1-366 was amplified by PCR and sub-cloned into the pET28a-LIC-C His vector, downstream of the poly-histidine coding region with M at the C-terminal region. The proteins were over-expressed in *E. coli* BL21 (DE3) pRARE2-V2R by the addition of 1 mM isopropyl-1-thio-D-galactopyranoside (IPTG) and incubated overnight at 15 ^{o}C. Harvested cells were re-suspended in 20 mM Tris buffer, pH 7.5, with 500 mM NaCl, 5 mM imidazole and 5% glycerol and flash frozen in presence of protease inhibitor. The cells were thawed and lysed chemically (CHAPS to final concentration of 0.5%, and 22.5 U/mL benzonase) followed by sonication at a frequency of 8.5 Hz with 10 s on and 10 s off. After clarification of the crude extract by high-speed centrifugation (16000 rpm for 1 h), the lysate was loaded onto a DE52 column and passed onto the Ni-NTA column. The column was washed and His–tagged protein was eluted by 20 mM Tris, pH 7.5, 500 mM NaCl, 5% glycerol, 50 mM and 250 mM imidazole, respectively. For KMT7, the protein was dialyzed against 20 mM Tris buffer, pH 7.5, and 500 mM NaCl. Next 4 mM DTT and 10% Glycerol were added to 90% pure KMT7 after concentration. The protein was stored at -80 °C after flash freezing in liquid nitrogen. For EHMT2, thrombin was used to cut the His-tag overnight, the cut protein was passed through an Ni-NTA column, and the flow through was loaded

onto a Superdex 200 16/60 column which was equilibrated with 20 mM Tris, pH 7.5 and 500 mM NaCl. Fractions with higher than 95% purity, as judged by SDS-PAGE, were pooled, concentrated and flash frozen. For KMT1B, thrombin was used to cut the His-tag overnight, the cut protein was diluted to 50 mM NaCl prior to injection onto a 6 mL Resource S cation exchange column which was pre-equilibrated with 3 column volume (CV) 10 mM Tris pH 6.8, followed by 3 CV of 10 mM Tris pH 6.8 containing 500 mM NaCl and 3CV of 10 mM Tris pH 6.8. The pure KMT1B eluted at around 150-300 mM NaCl. Pure fractions based on SDS-PAGE were pooled, concentrated and flash frozen.

For KDM3A, a DNA fragment encoding residues 515-1317, was amplified by PCR and sub-cloned into the SGC in-house pFB-CT10HF-LIC vector. Recombinant baculovirus was produced by transformation of DH10Bac cells. *Spodoptera frugiperda* (Sf9) insect cells in Sf-900 II SFM medium (Life Technologies) were infected with recombinant baculovirus and incubated for 72 h at 27 °C in shake flasks to over-express the protein. Harvested cells were suspended in buffer containing 50 mM HEPES (pH adjusted using KOH), pH 7.4, 300 mM KCl, 5 mM imidazole, 5% glycerol, 10 mM imidazole and protease inhibitor cocktail set VII (Calbiochem) and lysed by Dounce homogenization. The protein was purified by Ni-NTA chromatography on Sepharose 6 FF resin charged with nickel (GE Healthcare) followed by gel filtration on Superdex 200 column. The pure protein was stored in 20 mM HEPES, pH 7.4, 300 mM KCl and 5% glycerol at -80 °C after flash freezing.

For KDM4A, a DNA fragment encoding residues 1-359 was amplified by PCR and sub-cloned into the SGC in-house pNIC28-Bsa4 vector. The protein was over-expressed in *E. coli* BL21 (DE3) -R3-pRARE2 by the addition of 0.2 mM IPTG and incubated overnight at 18 °C. Harvested cells were frozen at -80 °C. The cells were thawed and suspended in buffer containing 50 mM HEPES, pH 7.5, 500 mM NaCl, 10 mM imidazole, protease inhibitor cocktail set III (Calbiochem) and 50 U of Benzonase (Merck Millipore) and lysed by high pressure homogenization (25 kpsi). The protein was purified by Ni-NTA chromatography on a 1 mL HisTrap FF Crude column (GE Healthcare) followed by ion exchange on a 1 mL HiTrap HP Q column (GE Healthcare). The pure protein was stored in 25 mM HEPES, pH 7.5, 500 mM NaCl, 5% glycerol at -80 °C after flash freezing.

KDM1A assay

The assay was performed in 384-well format. 60 nM KDM1A with or without compounds was incubated with 5 µM biotin-labeled H3K4me1(1-21) peptide in 50 mM Tris-HCl, pH 8.0, 0.01% Triton X-100 using an Agilent Bravo automated liquid handling platform. The reaction volume was 10 µl. The plate was covered by aluminum foil and incubated at room temperature for 30 min. The plate was then heated at 80 °C for 15 min in a water bath to denature KDM1A and was centrifuged at 2000 rpm at 4 °C for 5 min. KMT7 (final concentration 1 µM), DTT (5 mM) and tritiated SAM (0.75 µM) were added into sample wells. After 1 h, 1 mM cold SAM was added to quench the reaction and 40 µl buffer (20 mM Tris-HCl, pH 8.0) was added into the quenched samples. All samples were then transferred into a streptavidin/scintillant-coated microplate (Flashplate ® PLUS; Perkin Elmer Life Sciences), allowed to bind for 1 h, and then detected on a

TopCount NXT HTS (PerkinElmer). When testing pH effect on KDM1A, since KMT7 activity could be affected by pH, we first incubated KDM1A in buffers with different pH, and then adjusted the pH of reaction mixtures to pH 8.0 after heat shock. Effects of salt and other reagents were characterized in the same way. Salt or other reagents (DMSO, DTT, Triton X-100) were added into the tested wells at the beginning; and then adjusted to same concentrations after heat shock to make sure the observed effect was on KDM1A rather than KMT7. When testing RN-1 potency, different concentrations of RN-1 were pre-incubated with KDM1A for 30 min before peptide was added.

KDM3A assay

For screening compounds, 80 nM KDM3A was incubated with 2.5 μM biotin-labeled H3K9me2 (1-21), 20 μM Fe(II), 20 μM ascorbic acid , 2.5 μM 2-OG in 50 mM Tris-HCl, pH 7.0, 0.01% Triton X-100 in a 10 μl reaction volume at room temperature for 0.5 h in the presence of compounds or DMSO. Several wells were prepared without KDM3A as background. The plate was then heat-shocked at 80°C for 10 min. 5 mM DTT, 0.75 μM hot SAM, 0.1 μM EHMT2 were added into plates after centrifuging at 4 °C. 1 mM cold SAM was added to quench the reaction after 1 h. 40 μl of buffer (20 mM Tris-HCl, pH 8.0) was added into the quenched wells. Quenched reaction mixtures were transferred to a streptavidin/scintillant-coated microplate (Flashplate ® PLUS; Perkin Elmer Life Sciences), and allowed to bind for 1 h, and then detected on a TopCount NXT HTS (PerkinElmer).

KDM4A assay

In 10 µl reaction volume, 50 nM KDM4A was incubated with 5 µM biotin-labeled H3K9me3 (1-21), 20 µM Fe(II), 20 µM ascorbic acid, 5 µM 2-OG in 50 mM HEPES, pH 7.5, 0.01% Triton X-100 for 1 h at room temperature in the presence of compounds or DMSO. The plate was covered with aluminum foil tightly and heat shocked in a water bath at 80°C for 10 min. After centrifuging, 0.5 µM KMT1B, 5 mM DTT and 0.75 µM hot SAM were added into each reaction well. 1 mM cold SAM was used to quench KMT1B activity after 1 h reaction. 40 µl of buffer (20 mM Tris-HCl, pH 8.0) was added into the quenched samples, and all samples were then transferred into a streptavidin/scintillant-coated microplate (FlashPlate® PLUS: PerkinElmer Life Sciences). The amount of methylated peptide was quantified by tracing the radioactivity (counts per min) as measured after 1 h using a TopCount NXT HTS (PerkinElmer). When IOX1 was tested, KDM4A was pre-incubated with inhibitor for 15 min before addition of H3K9me3 (1-21) and 2-OG.

Kinetic Parameters determination

To determine the kinetic parameters, 25 nM of each demethylase enzyme was used in the reaction. The demethylase reaction time was reduced to 15 min to make sure the initial velocities were determined in the linear range. The apparent K_m^{app} for each substrate was determined by varying the concentration of that particular substrate and keeping the concentration of the other substrate(s) at saturation. After 15 min incubation at room temperature, the reactions were quenched by heating at 80°C for 10 min. The corresponding coupling enzyme and ^{3}H-SAM were added to each plate and the reactions were incubated at room temperature for 1 h. The reactions were then quenched by

addition of equal volume of 7.5 M guanidinium hydrochloride (Gu-HCl). 10 µL of quenched reaction mix was spotted onto streptavidin-coated membrane squares (SAM2® Biotin capture membrane, Promega). The membrane was washed three times with 2 M NaCl for two min each time, then with water three times for 30 s each. The membrane was dried at 50 ^{o}C for 1 h and then each spotted square was cut from the membrane and placed in a scintillation vial. The amount of methylated peptide was quantified by tracing the radioactivity (counts per min) as counted by a TriCarb liquid scintillation counter (Perkin Elmer Life Sciences). In order to ensure that the observed changes in activities upon varying substrate concentrations used in determining the KDM kinetic parameters were independent of methylation activities of the coupled enzymes, the HMT concentrations as well as the concentration of their substrates were kept constant and in excess. We also confirmed the linearity of all initial velocities used in determining the KDM kinetic parameters (Fig. S2).

Results

To evaluate the demethylation activity of KDMs, we coupled each KDM with a protein lysine methyltransferase (PKMT) that methylates the same lysine mark on the histone tail (KDM1A and KMT7; KDM3A and EHMT2; KDM4A and KMT1B) (Fig. 1). Each selected PKMT was able to generate the methylation state of the mark that was the substrate for the corresponding KDM and *vice versa*. In general, we used methylated peptides as substrates for KDMs and planned that removal of a methyl group by a KDM will be followed by methylation of the same mark by a methyltransferase in the presence of ^{3}H-SAM. In this manner, KDM activity is monitored by the incorporation of ^{3}H-

methyl group into the target peptide (Fig. 1). KDMs were heat inactivated before addition of PKMTs in each reaction.

KDM1A/KMT7 coupled SPA development

KDM1A removes monomethyl (me1) and dimethyl (me2) groups from H3K4, while KMT7 monomethylates the same mark. We used biotinylated H3K4me1 (1-21) as KDM1A substrate. The reaction mixtures were incubated for 1 h and KDM1A was heat inactivated. The product of the reaction, H3K4me0 (1-21) peptide, was used as a substrate for KMT7 using ^{3}H-SAM (Fig. 1). Methylation rates were determined as described in material and methods that reflect KDM1A activity since the only available substrate for KMT7 was demethylated peptide generated by KDM1A.

Optimum KDM1A activity was observed at pH 7.5-9.0 and low NaCl concentrations (Fig. S1). While most HMTs need reducing agents to be fully active [33, 34], no increase in KDM1A activity was observed in the presence of up to 15 µM DTT. Since reducing agents are necessary for KMT7 activity, 5 mM DTT was added to the reaction mixture after heat shock. DMSO concentrations up to 10% could be used without significantly affecting KDM1A activity (Fig. S1). Triton X-100 at concentrations below 0.02% had little effect on KDM1A activity (Fig. S1). We used the optimized conditions to determine the kinetic parameters for KDM1A ($K_m^{app}{}_{H3K4me1}$: 5 ± 1 µM; k_{cat}^{app}: 246 ± 12 h^{-1}) (Fig. 2A, Table 1), which are similar to reported result using same peptide substrate [35]. RN-1, an irreversible inhibitor of KDM1A [36], showed an IC_{50} value of 0.6 ± 0.05 µM in our

KDM1A/KMT7 coupled assay (Fig. 2B). We were able to perform this assay in 384-well format with a Z'-factor of 0.72 (Fig. S3) [37].

KDM3A/EHMT2 coupled SPA development

KDM3A (JMJD1A) is a histone demethylase that specifically demethylates H3K9. It preferentially demethylates mono- and dimethylated H3K9 residues, with a preference for dimethylated residue, while it has weak or no activity on trimethylated H3K9 [38]. We coupled KDM3A with EHMT2 that specifically mono- and dimethylates H3K9. In this assay, biotinylated H3K9me2 (1-21) was used as substrate (Fig. 1C). During the assay, the H3K9me2 (1-21) was demethylated by KDM3A into H3K9me1 or H3K9me0, which was then methylated by EHMT2 using ^{3}H-SAM. To obtain a reasonable signal to noise ratio, we used 100 nM EHMT2 (signal-to-noise of > 10) (Fig. S3). Signal in the absence of KDM3A was considered background and subtracted.

KDM3A showed optimum activity at pH 7.0 (Fig. S1). Similar to KDM1A, high concentration of NaCl reduced KDM3A activity; DMSO was tolerated up to 10% and DTT had little effect on KDM3A activity. High concentrations of Triton X-100 slightly reduced KDM3A activity (Fig. S1). Iron (II) and ascorbic acid at concentrations lower than 20 µM were used for KDM3A to reach maximum activity (Fig. S4).

Kinetic parameters for KDM3A were determined under the optimum assay conditions ($K_m^{app}{}_{H3K9me2(1-21)}$: 0.4 ± 0.1 µM; $K_m^{app}{}_{2\text{-}OG}$: 0.5 ± 0.1 µM; k_{cat}^{app} 198 ± 6 h^{-1}) (Fig. 3; Table 1). IOX1 (8-hydroxyquinoline-5-carboxylic acid) [20], a known KDM inhibitor also inhibited KDM3A with an IC_{50} value of 1 ± 0.1 µM (Fig. 3E; Table1). A Z'-factor of

0.7 was determined for performing this assay in 384-well format confirming robustness of this assay (Fig. S3).

KDM4A/KMT1B coupled SPA development

KDM4A is a histone demethylase that specifically demethylates H3K9 and H3K36. KDM4A demethylates trimethylated H3K9 and H3K36, while it has weak activity on mono- and dimethylated residues [39, 40]. So far, in all reported KDM4A kinetic studies and assay development, short peptides, H3K9me3 (1-15) or H3K9me3 (7-14) have been used as substrates [39-44]. At first, a short peptide H3K9me3 (1-15) was tested in our coupled assay. However, KDM4A showed very weak activity with estimated K_m of 70 μM and k_{cat} of 0.3 h^{-1}, which is similar to the previously reported result [41, 43]. However, we found that KDM4A showed much higher activity with longer peptide H3K9me3 (1-21) ($K_m^{app}{}_{H3K9me3(1-21)}$: 1.5 ± 0.3 μM; k_{cat} 108 ± 6 h^{-1}). Therefore, in the assay development for KDM4A, we used biotin labeled H3K9me3 (1-21) as substrate. In the crystal structure of KDM4A/H3K9me3 complex, only the interaction between H3 (7-14) and KDM4A were observed [40]. However, based on our results, residues after H3K14 may also contribute to the interaction between H3 and KDM4A.

KDM4A was coupled with KMT1B, which specifically trimethylates H3K9 (Fig. 1D). Since KMT1B showed no activity with H3K9me3 (1-21) and the assay had very low background (signal-to-noise ratio of >200), we used 0.5 μM KMT1B to obtain maximum signal.

KDM4A showed highest activity at pH 7.5 (Fig. S1). High concentration of NaCl and DTT reduced KDM4A activity. DMSO up to 10% had little effect on KDM4A activity.

High concentration of Triton X-100 was avoided to maximize KDM4A activity (Fig. S1). High concentrations of Iron (II) and ascorbic acid were used to increase KDM4A activity (Fig. S4). Kinetic parameters were also determined ($K_m^{app}{}_{H3K9me3(1-21)}$: 1.5 ± 0.3 µM; $K_m^{app}{}_{2\text{-}OG}$:10.5 ± 1.6 µM; k_{cat}^{app}: 108 ± 6 h^{-1}) (Fig. 3; Table1). KDM4A activity was also inhibited by IOX1 with an IC_{50} value of 4.0 ± 0.3 µM (Fig. 3F), which is comparable to the reported result by MALDI-TOF MS assay (1.7 µM) at similar 2OG concentration [20]. Z'-factor of 0.8 was obtained with IOX1 indicating suitability of this assay for screening in 384-well format as well (Fig. S3).

Discussion

When Zhang *et al* discovered KDMs (JKDM1A, JKDM2A, JKDM3A, etc) using a radioactive assay, nucleosomes or octamer was first methylated with different methyltransferases using tritiated SAM, and tritiated formaldehyde was detected after incubation with KDM fractions [17, 38, 45]. In this study, we use the reverse reaction sequence to test for KDM activity in which a demethylated substrate is subsequently methylated using ^{3}H-SAM. This sequence minimizes the manipulation of radioactive materials and also eliminates the generation of a volatile radioactive component (formaldehyde). Table 2 presents the advantages and disadvantages of the fluorescence-based, LS/MS-based and SPA assay formats.

Despite these advantages, compounds that interfere with coupled HMT activity would also show up as hits. HMT assays need to be considered as counter screens to identify these types of false positives when screening KDMs. In this study, the compounds tested (RN-1 and IOX1) showed no inhibition against the coupled HMTs (data not shown). For

compounds that inhibit both KDM and coupled HMT, a simple reverse coupled assay can be used for testing compounds inhibition potency only against KDMs. In this reversed assay, a peptide is first methylated by a HMT with hot SAM, and then a KDM and different concentrations of inhibitors are added to demethylate the methylated peptide after HMT is denatured by heat shock. In this reverse assay, only inhibition against KDM is monitored. For example, a potent in-house KMT7 inhibitor shows good inhibition in the KDM1A/KMT7 SPA. However, the compound shows no inhibition against KDM1A in the reversed KMT7/KDM1A assay in which the compound is added after KMT7 is denatured (data not shown).

Here, we report the development of a coupled KDM/HMT SPA for KDM1A, KDM3A, KDM4A, and in fact, the methods can be exploited for other KDMs with slight modifications. However, three factors should be taken into consideration for such assay development. First, an appropriate coupling HMT needs to be selected. The HMT's activity, selectivity, expression system and yield should be taken into consideration. For example, for KDM4A assay, both KMT1E and KMT1B could be used as coupled enzymes. Both enzymes showed high activity in the assay, however, KMT1E can only be expressed in Sf9 cells *via* a baculovirus expression system while KMT1B can be efficiently expressed in *E. coli*. Therefore, KMT1B was selected for KDM4A coupling SPA to reduce cost.

Secondly, peptide sequence and methylation status should be carefully selected. Since most of KDMs are active with tri-/dimethylated or mono-/dimethylated peptides, there are several peptides with different methylation states which could be used as substrates, and several HMTs could be used for the coupled methylation. In this condition, the effect

of peptide sequences and methylation states on KDM/HMT activity is very important. For example, in KDM4A assay, the k_{cat}^{app}/K_m^{app} with H3K9me3 (1-21) is over 5000 fold of that with H3K9me3 (1-15). KDM3A is also very active with H3K9me2 (1-21) while showing no activity with H3K9me2 (1-13). However, although longer peptides increase enzyme activity, it also may result in elevated background levels. For example, while background activity was low using H3K9me3 (1-21) as a substrate for KMT1B, it was significantly higher with H3K9me3 (1-25). Therefore, in the coupled KDM4A/KMT1B assay, H3K9me3 (1-21) was used as a substrate rather than H3K9me3 (1-25) or H3K9me3 (1-15).

Another example is KDM3A/EHMT2 assay. Higher background signal was observed using H3K9me2 (1-21) as a substrate for EHMT2. Considering the possibility that EHMT2 may have a residual activity with other available lysine residues, we synthesized a mutated H3K9me2 (1-21) with all lysine residues (except K9) replaced with alanine. However, while EHMT2 showed no activity with mutated H3K9me2 (1-21), KDM3A is also inactive with this peptide. So H3K9me2 (1-21) was chosen to be used by optimizing the EHMT2 concentration and buffers to produce high S/N. Therefore, the correct combination of peptides and HMTs is vital for this coupled assay.

Thirdly, when optimizing the coupled KDM/HMT assay, the effect of assay conditions on both HMT and KDM should be considered. For example, in the KDM4A/KMT1B assay, DTT can increase KMT1B activity; however, it greatly reduces KDM4A activity. Therefore, in the assay, DTT should be added after KMD4A denaturation instead of adding DTT at the beginning of the demthylation reaction.

In summary, we have described the development of three KDM/HMT coupled assays representing three different classes of KDMs. In each case, the optimization of conditions and reagents furnished robust assays which could be extended to encompass all members of the KDM family.

Acknowledgments

We thank Albina Bolotokova for preparing all peptides for the assays. The Structural Genomics Consortium is a registered charity (number 1097737) that receives funds from Bayer, Canadian Institutes of Health Research, Eli Lilly Canada, Genome Canada, GlaxoSmithKline, the Ontario Ministry of Economic Development and Innovation, the Novartis Research Foundation, Boehringer Ingelheim, Janssen, Pfizer, AbbVie, Takeda and the Wellcome Trust.

References:

[1] C.H. Arrowsmith, C. Bountra, P.V. Fish, K. Lee, M. Schapira, Epigenetic protein families: a new frontier for drug discovery, Nat. Rev. Drug. Discov., 11 (2012) 384-400.

[2] M. Tachibana, K. Sugimoto, M. Nozaki, J. Ueda, T. Ohta, M. Ohki, M. Fukuda, N. Takeda, H. Niida, H. Kato, Y. Shinkai, G9a histone methyltransferase plays a dominant role in euchromatic histone H3 lysine 9 methylation and is essential for early embryogenesis, Genes. Dev., 16 (2002) 1779-1791.

[3] X.J. Sun, J. Wei, X.Y. Wu, M. Hu, L. Wang, H.H. Wang, Q.H. Zhang, S.J. Chen, Q.H. Huang, Z. Chen, Identification and characterization of a novel human histone H3 lysine 36-specific methyltransferase, J. Biol. Chem., 280 (2005) 35261-35271.

[4] I. Hoffmann, M. Roatsch, M.L. Schmitt, L. Carlino, M. Pippel, W. Sippl, M. Jung, The role of histone demethylases in cancer therapy, Mol. Oncol., 6 (2012) 683-703.

[5] Y. Shi, F. Lan, C. Matson, P. Mulligan, J.R. Whetstine, P.A. Cole, R.A. Casero, Y. Shi, Histone demethylation mediated by the nuclear amine oxidase homolog LSD1, Cell, 119 (2004) 941-953.

[6] A. Scoumanne, X. Chen, The lysine-specific demethylase 1 is required for cell proliferation in both p53-dependent and -independent manners, J. Biol. Chem., 282 (2007) 15471-15475.

[7] M.M. Musri, M.C. Carmona, F.A. Hanzu, P. Kaliman, R. Gomis, M. Parrizas, Histone demethylase LSD1 regulates adipogenesis, J. Biol. Chem., 285 (2010) 30034-30041.

[8] S. Lv, W. Bu, H. Jiao, B. Liu, L. Zhu, H. Zhao, J. Liao, J. Li, X. Xu, LSD1 is required for chromosome segregation during mitosis, Eur. J. of Cell Biol., 89 (2010) 557-563.

[9] C.T. Foster, O.M. Dovey, L. Lezina, J.L. Luo, T.W. Gant, N. Barlev, A. Bradley, S.M. Cowley, Lysine-specific demethylase 1 regulates the embryonic transcriptome and CoREST stability, Mol. Cell. Biol., 30 (2010) 4851-4863.

[10] W.W. Tsai, T.T. Nguyen, Y. Shi, M.C. Barton, p53-targeted LSD1 functions in repression of chromatin structure and transcription in vivo, Mol. Cell. Biol., 28 (2008) 5139-5146.

[11] J. Huang, R. Sengupta, A.B. Espejo, M.G. Lee, J.A. Dorsey, M. Richter, S. Opravil, R. Shiekhattar, M.T. Bedford, T. Jenuwein, S.L. Berger, p53 is regulated by the lysine demethylase LSD1, Nature, 449 (2007) 105-108.

[12] R. Ueda, T. Suzuki, K. Mino, H. Tsumoto, H. Nakagawa, M. Hasegawa, R. Sasaki, T. Mizukami, N. Miyata, Identification of cell-active lysine specific demethylase 1-selective inhibitors, J. Amer. Chem. Soc., 131 (2009) 17536-17537.

[13] J. Wang, F. Lu, Q. Ren, H. Sun, Z. Xu, R. Lan, Y. Liu, D. Ward, J. Quan, T. Ye, H. Zhang, Novel histone demethylase LSD1 inhibitors selectively target cancer cells with pluripotent stem cell properties, Cancer Res., 71 (2011) 7238-7249.

[14] Y. Chen, W. Jie, W. Yan, K. Zhou, Y. Xiao, Lysine-specific histone demethylase 1 (LSD1): A potential molecular target for tumor therapy, Crit. Rev. Eukaryot. Gene Expr., 22 (2012) 53-59.

[15] J.T. Lynch, W.J. Harris, T.C. Somervaille, LSD1 inhibition: a therapeutic strategy in cancer?, Expert Opin Ther. Targets, 16 (2012) 1239-1249.

[16] H. Hou, H. Yu, Structural insights into histone lysine demethylation, Curr. Opin. Struct. Biol., 20 (2010) 739-748.

[17] R.J. Klose, E.M. Kallin, Y. Zhang, JmjC-domain-containing proteins and histone demethylation, Nat. Rev. Genet., 7 (2006) 715-727.

[18] L. Wang, J. Chang, D. Varghese, M. Dellinger, S. Kumar, A.M. Best, J. Ruiz, R. Bruick, S. Pena-Llopis, J. Xu, D.J. Babinski, D.E. Frantz, R.A. Brekken, A.M. Quinn, A. Simeonov, J. Easmon, E.D. Martinez, A small molecule modulates Jumonji histone demethylase activity and selectively inhibits cancer growth, Nat. Commun., 4 (2013) 2035.

[19] V. Yu, T. Fisch, A.M. Long, J. Tang, J.H. Lee, M. Hierl, H. Chen, P. Yakowec, R. Schwandner, R. Emkey, High-throughput TR-FRET assays for identifying inhibitors of LSD1 and JMJD2C histone lysine demethylases, J. Biomol. Screen., 17 (2012) 27-38.

[20] O.N. King, X.S. Li, M. Sakurai, A. Kawamura, N.R. Rose, S.S. Ng, A.M. Quinn, G. Rai, B.T. Mott, P. Beswick, R.J. Klose, U. Oppermann, A. Jadhav, T.D. Heightman, D.J. Maloney, C.J. Schofield, A. Simeonov, Quantitative high-throughput screening identifies 8-hydroxyquinolines as cell-active histone demethylase inhibitors, PLoS One, 5 (2010) e15535.

[21] S. Krishnan, E. Collazo, P.A. Ortiz-Tello, R.C. Trievel, Purification and assay protocols for obtaining highly active Jumonji C demethylases, Anal. Biochem., 420 (2012) 48-53.

[22] T.J. Wigle, L.M. Provencher, J.L. Norris, J. Jin, P.J. Brown, S.V. Frye, W.P. Janzen, Accessing protein methyltransferase and demethylase enzymology using microfluidic capillary electrophoresis, Chem. Biol., 17 (2010) 695-704.

[23] C.J. Hastie, H.J. McLauchlan, P. Cohen, Assay of protein kinases using radiolabeled ATP: a protocol, Nat. Protoc., 1 (2006) 968-971.

[24] H. Ma, S. Deacon, K. Horiuchi, The challenge of selecting protein kinase assays for lead discovery optimization, Expert Opin. Drug. Discov., 3 (2008) 607-621.

[25] T.C. Turek-Etienne, E.C. Small, S.C. Soh, T.A. Xin, P.V. Gaitonde, E.B. Barrabee, R.F. Hart, R.W. Bryant, Evaluation of fluorescent compound interference in 4 fluorescence polarization assays: 2 kinases, 1 protease, and 1 phosphatase, J. Biomol. Screen., 8 (2003) 176-184.

[26] M. Plant, T. Dineen, A. Cheng, A.M. Long, H. Chen, K.A. Morgenstern, Screening for lysine-specific demethylase-1 inhibitors using a label-free high-throughput mass spectrometry assay, Anal. Biochem., 419 (2011) 217-227.

[27] B.L. Ackermann, M.J. Berna, J.A. Eckstein, L.W. Ott, A.K. Chaudhary, Current applications of liquid chromatography/mass spectrometry in pharmaceutical discovery after a decade of innovation, Annu. Rev. Anal. Chem. (Palo Alto Calif), 1 (2008) 357-396.

[28] T. Takagi, D. Shum, M. Parisi, R.E. Santos, C. Radu, P. Calder, Z. Rizvi, M.G. Frattini, H. Djaballah, Comparison of luminescence ADP production assay and radiometric scintillation proximity assay for Cdc7 kinase, Comb. Chem. High Throughput Screen., 14 (2011) 669-687.

[29] Y.W. Park, R.T. Cummings, L. Wu, S. Zheng, P.M. Cameron, A. Woods, D.M. Zaller, A.I. Marcy, J.D. Hermes, Homogeneous proximity tyrosine kinase assays: scintillation proximity assay versus homogeneous time-resolved fluorescence, Anal. Biochem., 269 (1999) 94-104.

[30] C.J. Sneeringer, M.P. Scott, K.W. Kuntz, S.K. Knutson, R.M. Pollock, V.M. Richon, R.A. Copeland, Coordinated activities of wild-type plus mutant EZH2 drive tumor-

associated hypertrimethylation of lysine 27 on histone H3 (H3K27) in human B-cell lymphomas, Proc. Natl. Acad. Sci. U S A, 107 (2010) 20980-20985.

[31] J. Wu, N. Xie, Y. Feng, Y.G. Zheng, Scintillation proximity assay of arginine methylation, J. Biomol. Screen., 17 (2012) 237-244.

[32] A.D. Ferguson, N.A. Larsen, T. Howard, H. Pollard, I. Green, C. Grande, T. Cheung, R. Garcia-Arenas, S. Cowen, J. Wu, R. Godin, H. Chen, N. Keen, Structural basis of substrate methylation and inhibition of SMYD2, Structure, 19 (2011) 1262-1273.

[33] K.Y. Horiuchi, M.M. Eason, J.J. Ferry, J.L. Planck, C.P. Walsh, R.F. Smith, K.T. Howitz, H. Ma, Assay development for histone methyltransferases, Assay Drug Dev. Technol., 11 (2013) 227-236.

[34] V.M. Richon, D. Johnston, C.J. Sneeringer, L. Jin, C.R. Majer, K. Elliston, L.F. Jerva, M.P. Scott, R.A. Copeland, Chemogenetic analysis of human protein methyltransferases, Chem. Biol. Drug Des., 78 (2011) 199-210.

[35] F. Forneris, C. Binda, M.A. Vanoni, E. Battaglioli, A. Mattevi, Human histone demethylase LSD1 reads the histone code, J. Biol. Chem., 280 (2005) 41360-41365.

[36] R. Neelamegam, E.L. Ricq, M. Malvaez, D. Patnaik, S. Norton, S.M. Carlin, I.T. Hill, M.A. Wood, S.J. Haggarty, J.M. Hooker, Brain-penetrant LSD1 inhibitors can block memory consolidation, ACS Chem. Neurosci., 3 (2011) 120-128.

[37] J.H. Zhang, T.D. Chung, K.R. Oldenburg, A Simple Statistical Parameter for Use in Evaluation and Validation of High Throughput Screening Assays, J. Biomol. Screen., 4 (1999) 67-73.

[38] K. Yamane, C. Toumazou, Y. Tsukada, H. Erdjument-Bromage, P. Tempst, J. Wong, Y. Zhang, JHDM2A, a JmjC-containing H3K9 demethylase, facilitates transcription activation by androgen receptor, Cell, 125 (2006) 483-495.

[39] J.R. Whetstine, A. Nottke, F. Lan, M. Huarte, S. Smolikov, Z. Chen, E. Spooner, E. Li, G. Zhang, M. Colaiacovo, Y. Shi, Reversal of histone lysine trimethylation by the JMJD2 family of histone demethylases, Cell, 125 (2006) 467-481.

[40] S.S. Ng, K.L. Kavanagh, M.A. McDonough, D. Butler, E.S. Pilka, B.M. Lienard, J.E. Bray, P. Savitsky, O. Gileadi, F. von Delft, N.R. Rose, J. Offer, J.C. Scheinost, T. Borowski, M. Sundstrom, C.J. Schofield, U. Oppermann, Crystal structures of histone demethylase JMJD2A reveal basis for substrate specificity, Nature, 448 (2007) 87-91.

[41] L. Hillringhaus, W.W. Yue, N.R. Rose, S.S. Ng, C. Gileadi, C. Loenarz, S.H. Bello, J.E. Bray, C.J. Schofield, U. Oppermann, Structural and evolutionary basis for the dual substrate selectivity of human KDM4 histone demethylase family, J. Biol. Chem., 286 (2011) 41616-41625.

[42] Z. Chen, J. Zang, J. Kappler, X. Hong, F. Crawford, Q. Wang, F. Lan, C. Jiang, J. Whetstine, S. Dai, K. Hansen, Y. Shi, G. Zhang, Structural basis of the recognition of a methylated histone tail by JMJD2A, Proc. Natl. Acad. Sci. U S A, 104 (2007) 10818-10823.

[43] J.F. Couture, E. Collazo, P.A. Ortiz-Tello, J.S. Brunzelle, R.C. Trievel, Specificity and mechanism of JMJD2A, a trimethyllysine-specific histone demethylase, Nat. Struct. Mol. Biol., 14 (2007) 689-695.

[44] B. Cascella, L.M. Mirica, Kinetic analysis of iron-dependent histone demethylases: alpha-ketoglutarate substrate inhibition and potential relevance to the regulation of histone demethylation in cancer cells, Biochemistry, 51 (2012) 8699-8701.

[45] Y. Tsukada, J. Fang, H. Erdjument-Bromage, M.E. Warren, C.H. Borchers, P. Tempst, Y. Zhang, Histone demethylation by a family of JmjC domain-containing proteins, Nature, 439 (2006) 811-816.

Table 1

Kinetic constants and Z' for 3 KDMs

Enzyme	K_m^{app} (μM)		k_{cat}^{app} (h^{-1})	k_{cat}^{app}/K_m^{app} ($min^{-1}μM^{-1}$)	Z'
	2-OG	Peptide			
KDM1A	N/A	5.0 ± 1.0	246 ± 12	0.9 ± 0.2	0.72
KDM3A	0.4 ± 0.1	0.5 ± 0.1	198 ± 6	8.3 ± 0.2	0.70
KDM4A	10.5 ± 1.6	1.5 ± 0.3	108 ± 6	1.2 ± 0.1	0.80

Table 2

Advantages/disadvantages of various KDM assay formats

	Advantages	Disadvantages
Fluorescence-based assay	• High-throughput • No separation step • Low cost	• Sensitive to fluorescence interference from compounds • May need specific antibody and labeling
Mass spectrometry assay	• Label –free • Less sensitive to interference from compounds	• Instrument capacity is about 1/5 of fluorescence reader [26] • Product separation by chromatography required • High cost of mass spectrometer
Coupled SPA	• High-throughput • No separation step • Less sensitive to interference from compounds	• Need Coupled enzymes • Need decoupling assay for hit validation

Figure legends:

Fig. 1. Mechanism of coupled KDM/HMT scintillation proximity assay (SPA). (A) Phylogenetic tree of KDMs. Squares indicate three KDMs for which coupled assays were

developed. (B) Scheme of coupled KDM1A/KMT7 SPA; (C) Scheme of coupled KDM3A/EHMT2 SPA; (D) Scheme of coupled KDM4A/KMT1B SPA.

Fig. 2. KDM1A assay development. (A) Determination of K_m^{app} for H3K4me1; (B) Dose-response inhibition profile of KDM1A by RN-1.

Fig. 3. KDM3A and KDM4A assay development. (A) Determination of K_m^{app} for H3K9me2 with KDM3A; (B) Determination of K_m^{app} for 2-OG with KDM3A; (C) Determination of K_m^{app} for H3K9me3 with KDM4A; (D) Determination of K_m^{app} for 2-OG with KDM4A; (E) Dose-dependent inhibition of KDM3A by IOX1; (F) Dose-dependent inhibition of KDM4A by IOX1.

Development of a scintillation proximity assay for histone demethylases

Wenyu Yu[1], Mohammad S. Eram[1], Taraneh Hajian[1], Aleksandra Szykowska[3], Nicola Burgess-Brown[3], Masoud Vedadi[1,2] and Peter J. Brown[1*]

[1]Structural Genomics Consortium, University of Toronto, 101 College Street, Toronto, ON M5G 1L7, Canada

[2]Department of Pharmacology and Toxicology, University of Toronto, 1 King's College Circle, Toronto, Ontario, M5S 1A8, Canada.

[3]Structural Genomics Consortium, University of Oxford

Supplementary figures:

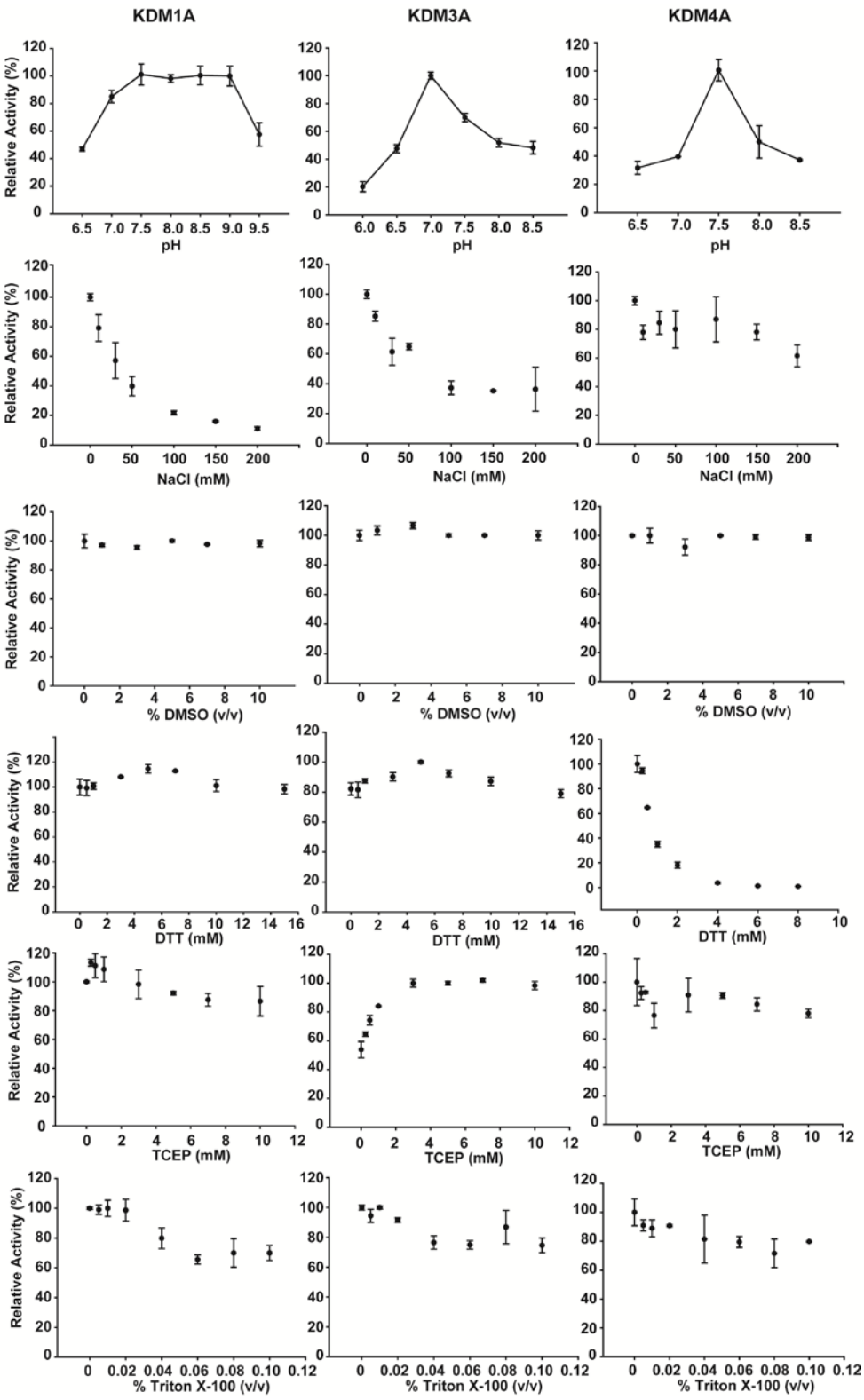

Figure S1. Effect of pH and additives on activity of KDMs. Effect of pH, NaCl, DMSO, DTT, and Triton X-100 on activity of KDM1A, KDM3A and KDM4A were assessed as described in Material and Methods. Experiments were performed in triplicate.

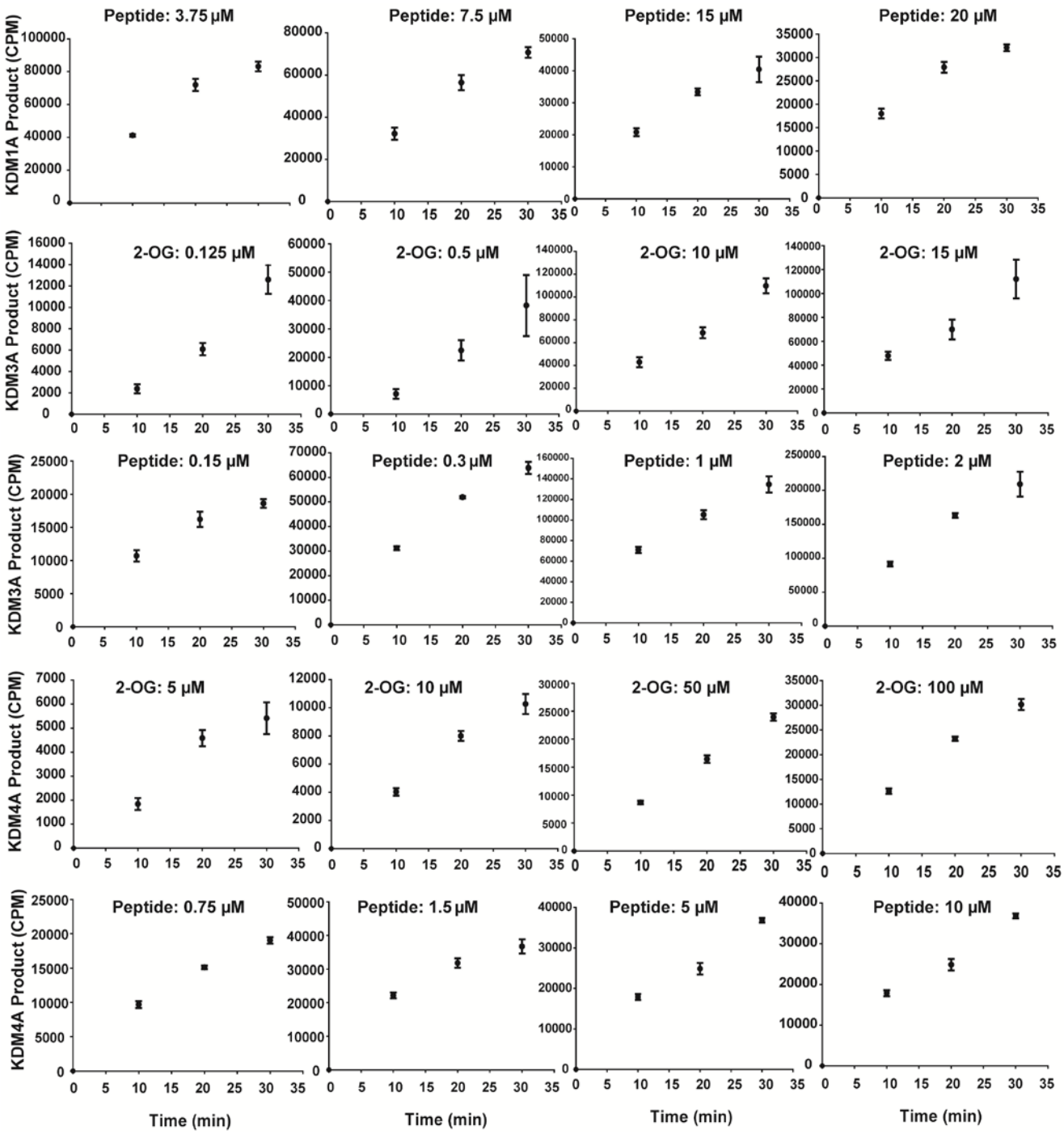

Figure S2. Linearity of initial velocities. The linearity of the initial velocities at different concentrations of substrates (below Km, around Km, and two above Km) were assessed and confirmed for a period of 30 min for KDM1A, KDM3A and KDM4A. In all experiments, 15 min enzymatic reaction time was used to make sure the values were determined within the linear range.

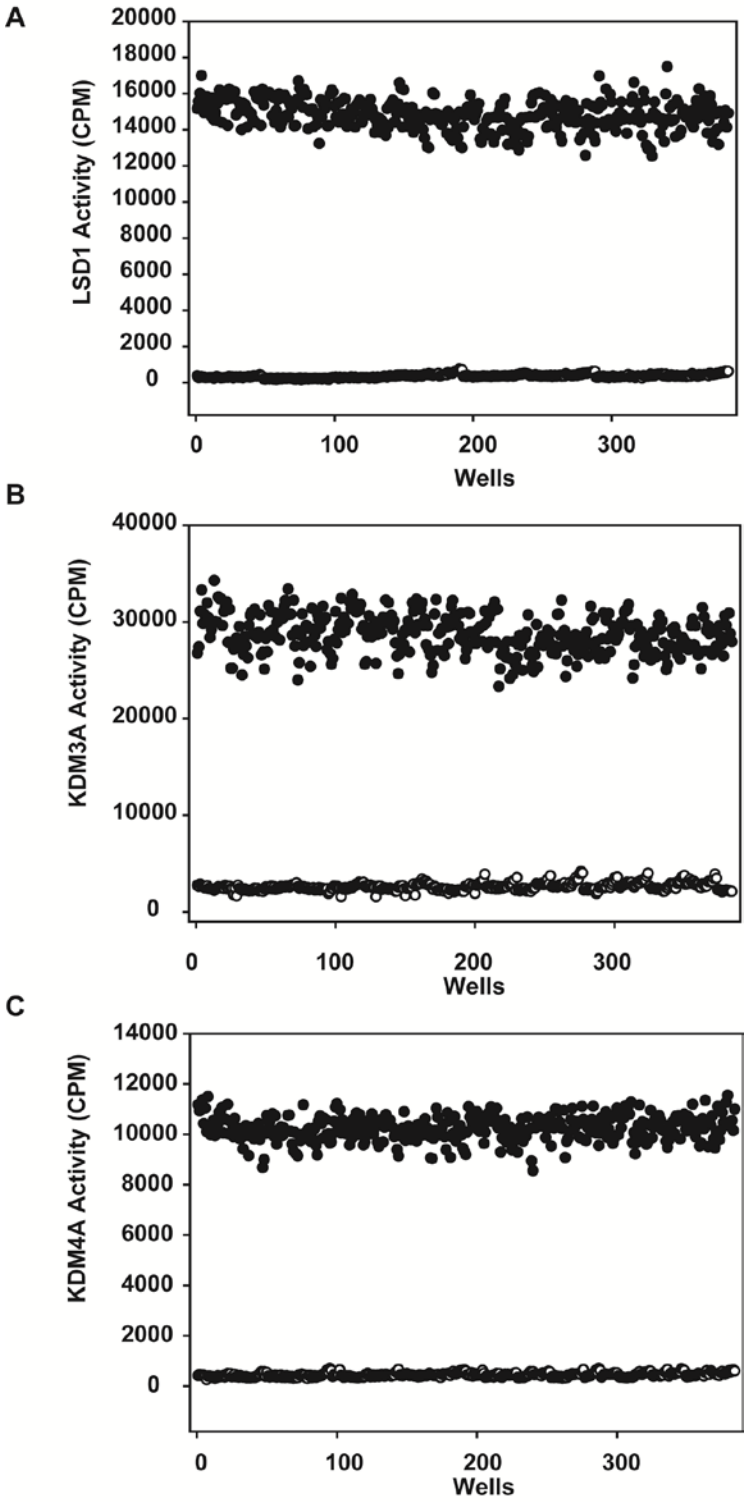

Figure S3. Z'-Factor determination. Z'-Factors were determined in the presence (opened circle) and absence (filled circle) of inhibitors for (A) KDM1A screening with RN-1; (B) KDM3A and (C) KDM4A with IOX1.

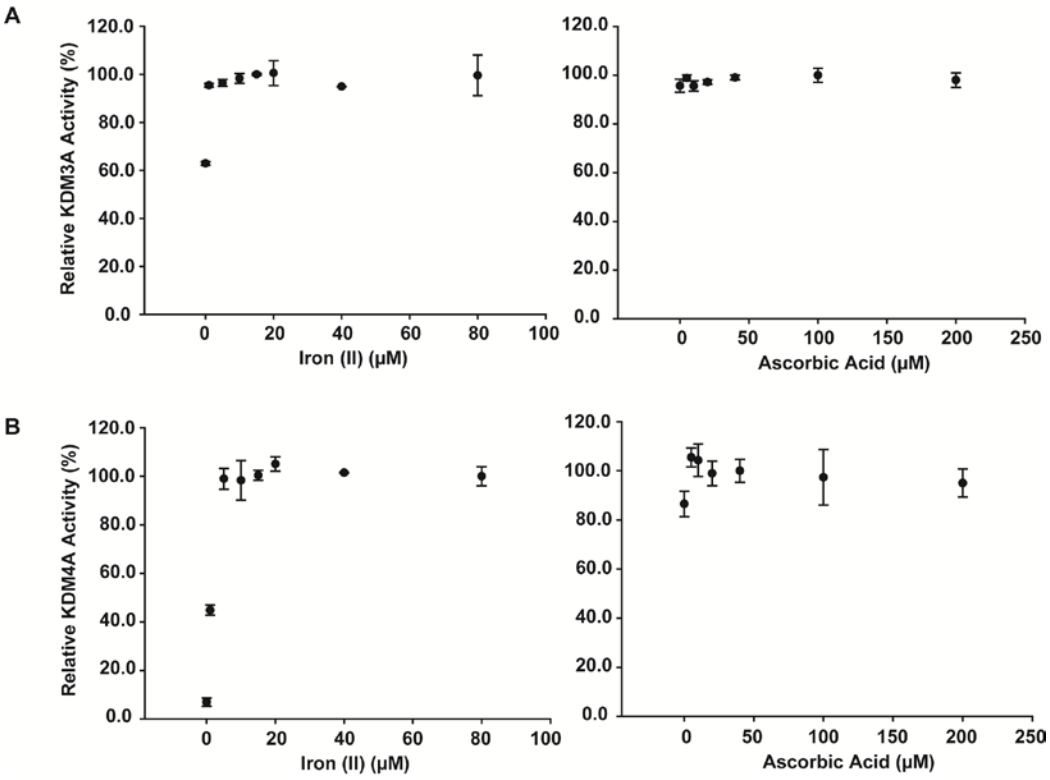

Figure S4. Effect of Iron (II) and ascorbic acid on KDM activity. Effect of Iron (II) and ascorbic acid on activity of (A) KDM3A and (B) KDM4A were assessed as described in Material and Methods. Experiments were performed in triplicate.